Electronic Supplementary Material (ESI) for Materials Horizons.

Supplementary Information

A chiral covalent organic frameworks (COFs) nanozyme with ultrahigh enzymatic activity

Ya Zhou, [a,b] *Yue Wei,* [a,b] *Jinsong Ren,* [a,b] *and Xiaogang Qu** [a,b]

[a] Laboratory of Chemical Biology and State Key Laboratory of Rare Earth Resource Utilization, Changchun Institute of Applied Chemistry, Chinese Academy of Sciences, Changchun, Jilin 130022, P. R. China.

[b] School of Applied Chemistry and Engineering, University of Science and Technology of China, Hefei, Anhui 230026 P. R. China.

Experimental Section

1. Materials. 2,2'-Azinobis(3-ethylbenzothiazoline-6-sulfonate) (ABTS) and iron(III) chloride hexahydrate, L-dopa, D-dopa, L-tyrosinol and D-tyrosinol were purchased from Sigma-Aldrich. 3-aminopropyltriethoxysilane (APTES) was obtained from Alfa Aesar. 1,4-Phthalaldehyde (TPA), glycidol (Glc), L-histidine (L-His), D-histidine (D-His), L-Alanine (L-Ala), L-tyrosine and D-tyrosine were purchased from Shanghai Macklin Biochemical Co., Ltd. (Shanghai, China). H_2O_2, N,N-dimethylformamide (DMF), acetone, 1,2-dichlorobenzene (o-DCB) and butyl alcohol (BuOH) were obtained from Beijing Chemicals (Beijing, China). 5,10,15,20-tetrakis(4'-tetraphenylamino) porphyrin (ATPP) and 2,5-dihydroxyterephthalaldehyde (DHA) were obtained from Jilin Chinese Academy of Sciences - Yanshen Technology Co., Ltd (Jilin, China). All other reagents were of analytical reagent grade, and used as received. Ultrapure water (18.2 MU; Millpore Co., USA) was used throughout the experiment.

2. Measurements and characterizations. The UV-vis absorption spectra were measured by a Jasco V550 UV/Visible spectrophotometer (JASCO International Co., Ltd., Tokyo, Japan). Fluorescence spectra were measured on a JASCO FP-6500 spectrofluorometer with a water bath to control the temperature. All spectra were carried out in a cell with 1.0 cm path length. CD spectra were carried out by a JASCO J-810 spectropolarimeter in a 5 mm path length quartz cell. Fourier transform infrared (FTIR) characterization was measured on a BRUKE Vertex 70 FT-IR spectrometer. The samples were thoroughly ground with exhaustively dried KBr. A FEI TECNAI

G2 20 high-resolution transmission electron microscope operating at 200 kV was applied to record the transmission electron microscopy (TEM) images. The X-ray diffraction (XRD) pattern were recorded by a D8 Advance Powder X-ray Diffractometer with CuKa radiation. The operation voltage and current were 40 kV and 40 mA, respectively. N_2 adsorption-desorption isotherms were measured by a Micromeritics ASAP 2020M automated sorption analyzer. The pore size was determined following the BJH method.

3. Synthesis of Fe-ATPP. ATPP (100 mg) and anhydrous ferric chloride (250mg) were added to anhydrous DMF (15 mL) under a nitrogen atmosphere. After being stirred at 150 °C for 4 h, cold water was added and then filtered. The precipitate was dissolved in CH_2Cl_2 and washed with pure water. The organic layer was dried with Na_2SO_4 and the solvent was evaporated in *vacuo* to give Fe-ATPP. MALDI-TOF MS: calcd. for $C_{44}H_{34}N_8Fe$ $[M+H]^+$: 731.34; found m/z 728.3.

4. Synthesis of Fe-COF and B-COF. Fe-COF and B-COF was synthesized following a previously reported procedure.[1] Fe-ATPP for Fe-COF or ATPP for B-COF (0.022 mmol) was dissolved in o-DCB/BuOH (0.5 mL/0.5 mL) in a Pyrex tube (10 mL), following by the addition of TPA (0.044 mmol) and acetic acid (3 M, 0.1 mL). The mixture was degassed by three freeze–pump–thaw cycles before sealed off. The tube was then heated at 120 °C for 3 days. The precipitate was separated *via* centrifuge, washed with THF and acetone. The powder was dried under vacuum overnight to give the corresponding COFs.

5. Synthesis of L-His$_x$@Fe-COF. L-His$_x$@Fe-COF was prepared according to the

literature.[1,2] Fe-ATPP (0.022 mmol) and DHA/TPA (total 0.044 mmol) at different molar ratios of 100/0, 75/25, 50/50, 25/75 was dissolved in o-DCB/BuOH (0.5 mL/0.5 mL) with acetic acid (3 M, 0.1 mL) in a Pyrex tube. The mixture was degassed by three freeze–pump–thaw cycles. After that the tube was sealed off and heated at 120 °C for 3 days. The precipitate was separated and washed with THF and acetone. The powder was dried under vacuum overnight. The obtained HO_x@Fe-COF (20mg) was dispersed in 10 mL of 0.1M $NaHCO_3$ solution. After sonication for 5 min, 250 μL of Glc was added and the mixture was heated at 100 °C for 24 h. The precipitate was then separated by centrifugation and washed with EtOH and toluene. Then the precipitate was dispersed in 10 mL of toluene and sonicated under N_2 atmosphere, following by the addition of APTES (150 μL). The mixture was refluxed under N_2 atmosphere for overnight. The precipitate was separated by centrifugation and washed with EtOH and aq. DMSO (1:1). 10 mg of L-His and 3mg EDC·HCl was added to 15 mL of aq. DMSO (1:1) and incubated for 3 h under dark condition. 3mg of NHS and the obtained product was added dropwise. The mixture was stirred for overnight under dark. Finally the product was centrifuged, washed with aq. DMSO, water, EtOH and dried under vacuum overnight to give the corresponding COFs.

6. Synthesis of L-Ala@Fe-COF and D-His@Fe-COF. Synthesis of L-Ala@Fe-COF and D-His@Fe-COF was based on HO_{50}@Fe-COF and HO_{75}@Fe-COF, respectively. The method was same with the synthesis corresponding L-His_x@Fe-COF while the L-His was replaced by L-Ala and D-His, respectively. The characterizations of L-Ala@Fe-COF and D-His@Fe-COF was shown in Fig. S19.

7. Bioassay. Kinetic measurements were carried out by using the time course mode to monitor the absorbance change of ABTS at 415 nm or dopa at 475 nm or tyrosinol at 320 nm. The kinetic measurements for tyrosine were carried out according to the reported procedure.[3] Experiments were conducted using 0.9 μg mL^{-1} COF with 2.5 mM ABTS or 500 μM dopa/tyrosinol as substrate in 500 μL buffer solutions (25 mM Na_2HPO_4, pH 4.0, 37 °C) with 50 mM H_2O_2, unless otherwise stated. The kinetic parameters were analyzed according to the Michaelis-Menten model: $\nu = V_{max}[S]/(K_m+[S])$, where ν is the initial velocity, V_{max} is the maximal reaction velocity, and [S] refers to the concentration of substrate. k_{cat} was calculated according to the equation: $k_{cat}=V_{max}/[E]$, where [E] refers to the concentration of catalyst.[4,5] The comparison of catalytic activity for different nanozymes and enzyme was estimated according the ratio of their k_{cat}/K_m values.

8. Measurement of activation energy. The activation energies (E_a) was calculated according to the Arrhenius equation:[4,6] $\ln(\nu) = A-E_a/R\times1/T$, where A is the frequency factor, R is the gas constant and T is the absolute temperature (K).

9. Dialysis. 1 ml of different COFs nanozymes (1 mg mL^{-1}) was dialyzed against a 10 ml solution containing a 1:1 mixture of dopa (2.5 mM). After 24 h dialysis, circular dichroism (CD) spectra of the dialysate solutions were measured to determine the enrichment of particular enantiomeric forms.[7]

Table S1. Kinetic parameters for catalytic decomposition of H_2O_2 by Fe-COF, L-His_{50}@Fe-COF or L-Ala@Fe-COF.

Nanozyme	[E] (M)	Substrate	K_m [mM]	k_{cat} [10^4 s^{-1}]	k_{cat}/K_m [10^6 s^{-1} M^{-1}]
Fe-COF	3.5×10^{-12}	H_2O_2	34.91±1.88	2.36±0.12	0.68
L-His_{50}@Fe-COF	3.5×10^{-12}	H_2O_2	3.32±0.14	5.95±0.22	17.92
L-Ala@Fe-COF	3.5×10^{-12}	H_2O_2	27.22±1.17	2.51±0.07	0.92

Table S2. Kinetic parameters for catalytic decomposition of H_2O_2 by L-His_x@Fe-COF or HRP.

Nanozyme	[E] (M)	Substrate	K_m [mM]	k_{cat} [10^4 s^{-1}]	k_{cat}/K_m [10^6 s^{-1} M^{-1}]
L-His_{25}@Fe-COF	3.5×10^{-12}	H_2O_2	8.89±0.58	3.77±0.32	4.24
L-His_{50}@Fe-COF	3.5×10^{-12}	H_2O_2	3.32±0.14	5.95±0.22	17.92
L-His_{75}@Fe-COF	3.5×10^{-12}	H_2O_2	2.04±0.11	7.23±0.36	35.44
L-His_{100}@Fe-COF	3.5×10^{-12}	H_2O_2	1.90±0.07	5.59±0.18	29.42
HRP	5.2×10^{-12}	H_2O_2	10.58±1.32	1.72±0.09	1.63

[E]: Concentrations of the corresponding nanozymes or enzyme.

Table S3. Kinetic parameters for catalytic oxidation of dopa enantiomers by Fe-COF, L-Ala@Fe-COF, L-His_{75}@Fe-COF or D-His@Fe-COF.

Nanozyme	Substrate	K_m [μM]	k_{cat} [10^4 s^{-1}]	k_{cat}/K_m [10^6 s^{-1} M^{-1}]	Select factor
Fe-COF	L-dopa	740.88±26.83	0.73±0.02	9.85	1.04
Fe-COF	D-dopa	764.06±69.11	0.78±0.04	10.21	
L-Ala@Fe-COF	L-dopa	665.80±82.03	0.85±0.04	12.77	1.11
L-Ala@Fe-COF	D-dopa	721.44±112.91	0.83±0.06	11.50	
L-His_{75}@Fe-COF	L-dopa	273.22±59.31	1.48±0.12	54.17	1.64
L-His_{75}@Fe-COF	D-dopa	396.89±29.68	1.31±0.04	33.01	
D-His@Fe-COF	L-dopa	417.79±42.23	1.25±0.05	29.92	1.51
D-His@Fe-COF	D-dopa	326.5±30.58	1.48±0.07	45.32	

Table S4. Kinetic parameters for catalytic oxidation of dopa enantiomers by L-His_x@Fe-COF.

Nanozyme	Substrate	K_m [μM]	k_{cat} [10^4 s^{-1}]	k_{cat}/K_m [10^6 s^{-1} M^{-1}]	Select factor
L-His_{25}@Fe-COF	L-dopa	355.99±54.38	1.09±0.06	29.78	1.28
L-His_{25}@Fe-COF	D-dopa	433.83±62.36	1.01±0.05	23.28	
L-His_{50}@Fe-COF	L-dopa	307.71±47.86	1.30±0.05	42.25	1.55
L-His_{50}@Fe-COF	D-dopa	419.27±71.71	1.14±0.08	27.19	
L-His_{75}@Fe-COF	L-dopa	273.22±59.31	1.48±0.12	54.17	1.64
L-His_{75}@Fe-COF	D-dopa	396.89±29.68	1.31±0.04	33.01	
L-His_{100}@Fe-COF	L-dopa	255.12±30.07	1.33±0.07	52.13	1.86
L-His_{100}@Fe-COF	D-dopa	388.61±37.51	1.09±0.04	28.05	

Concentrations of the all nanozymes are 3.5×10^{-12} M.

Table S5. Kinetic parameters for catalytic oxidation of tyrosinol enantiomers by Fe-COF, L-Ala@Fe-COF, L-His_{100}@Fe-COF or D-His@Fe-COF.

Nanozyme	Substrate	K_m [mM]	k_{cat} [10^4 s^{-1}]	k_{cat}/K_m [10^6 s^{-1} M^{-1}]	Select factor
Fe-COF	L-tyrosinol	1.27±0.07	0.80±0.04	6.30	1.04
Fe-COF	D-tyrosinol	1.25±0.12	0.82±0.05	6.56	
L-Ala@Fe-COF	L-tyrosinol	1.03±0.11	1.00±0.04	0.97	1.13
L-Ala@Fe-COF	D-tyrosinol	1.11±0.12	0.95±0.05	0.86	
L-His_{100}@Fe-COF	L-tyrosinol	0.66±0.11	1.57±0.09	23.79	1.72
L-His_{100}@Fe-COF	D-tyrosinol	0.94±0.09	1.30±0.07	13.83	
D-His@Fe-COF	L-tyrosinol	0.95±0.10	1.18±0.05	12.42	1.53
D-His@Fe-COF	D-tyrosinol	0.76±0.08	1.44±0.05	18.95	

Concentrations of the all nanozymes are 3.5×10^{-12} M.

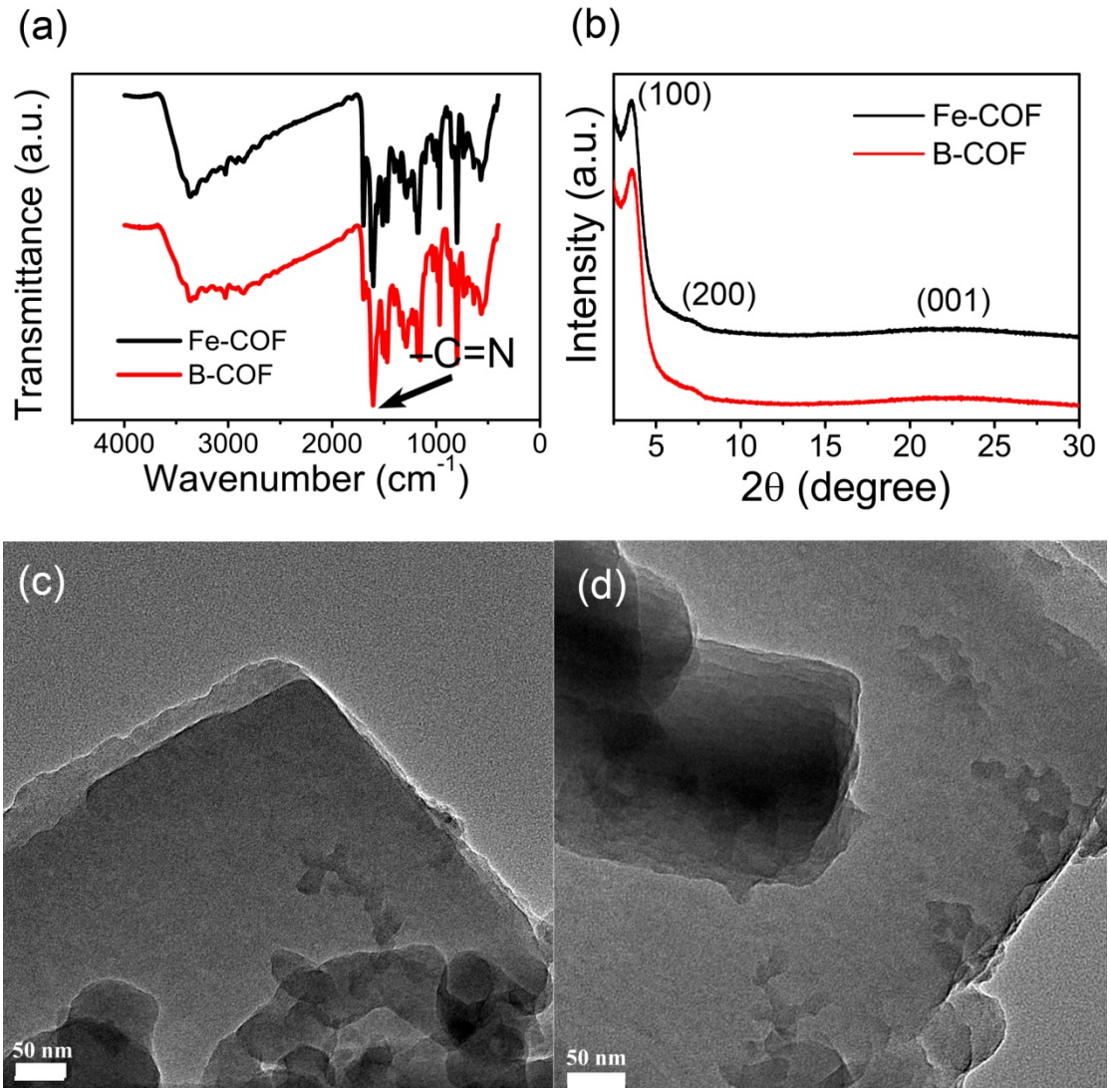

Fig. S1. (a) FTIR spectra of Fe-COF and B-COF. (b) XRD pattern of Fe-COF and B-COF. TEM images of (c) Fe-COF and (d) B-COF.

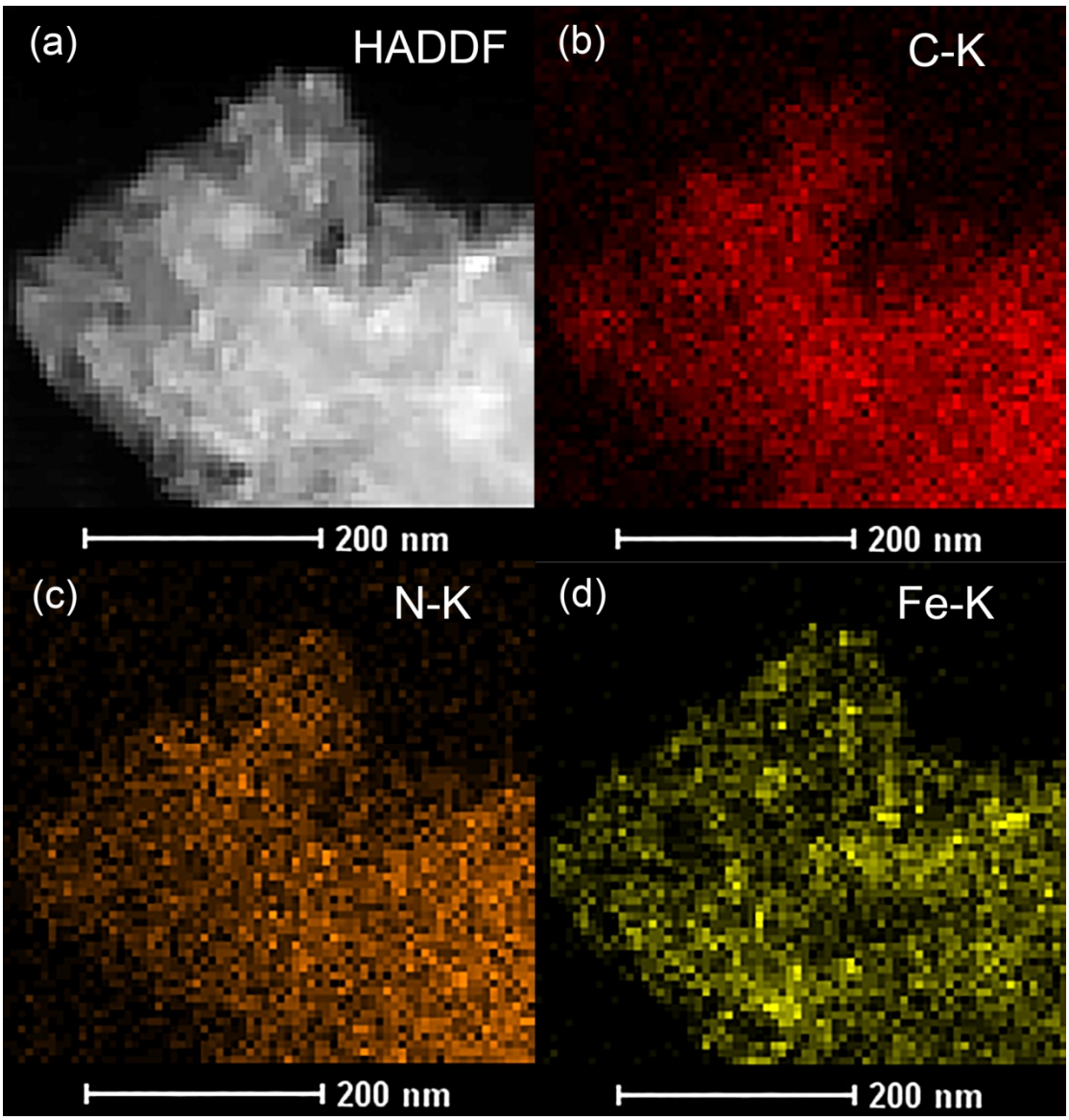

Fig. S2. TEM elemental mappings of Fe-COF.

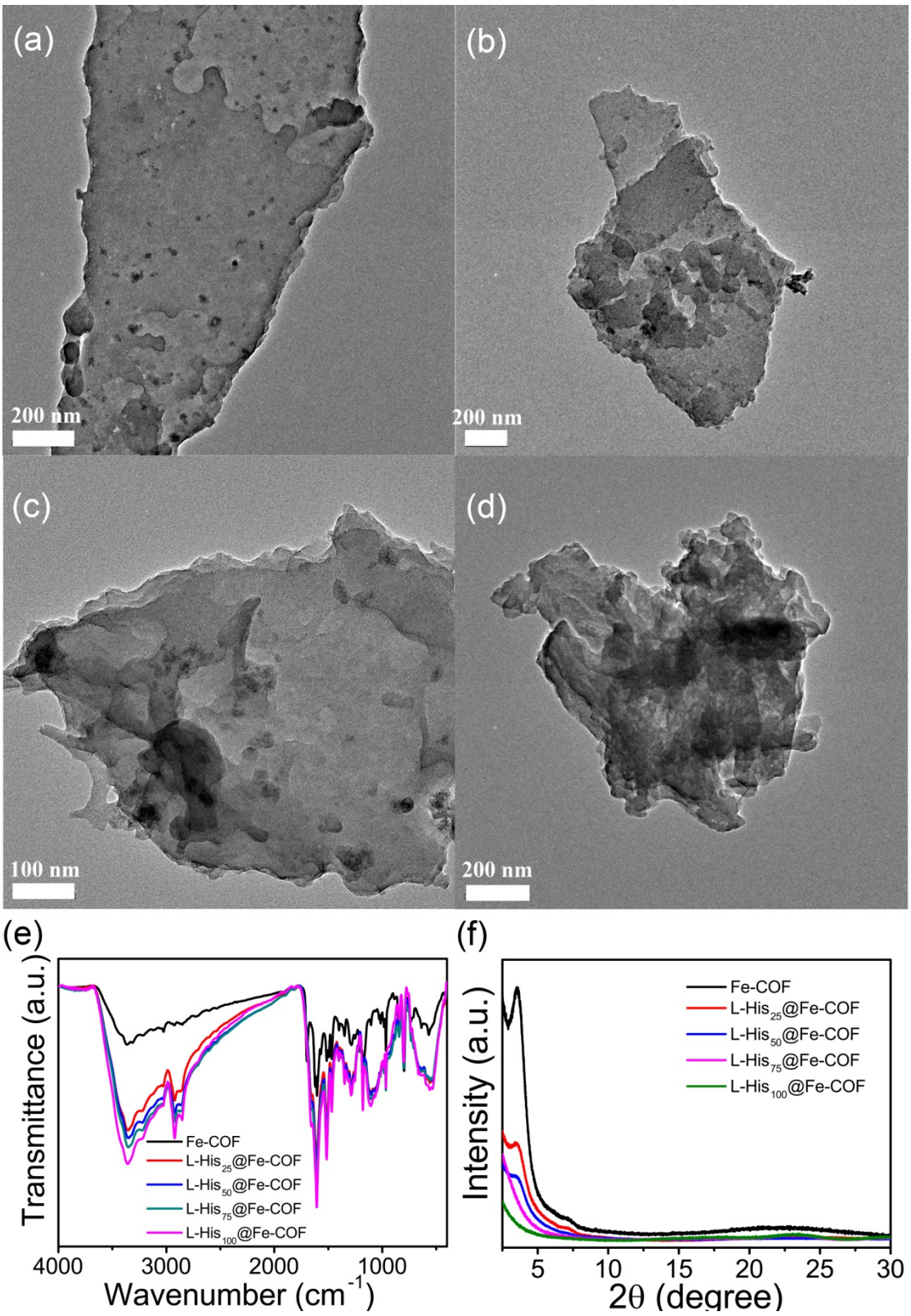

Fig. S3. TEM images of (a) L-His$_{25}$@Fe-COF, (b) L-His$_{50}$@Fe-COF, (c) L-His$_{75}$@Fe-COF and (d) L-His$_{100}$@Fe-COF. (e) FTIR spectra of Fe-COF and L-His$_x$@Fe-COF. (f) XRD pattern of Fe-COF and L-His$_x$@Fe-COF.

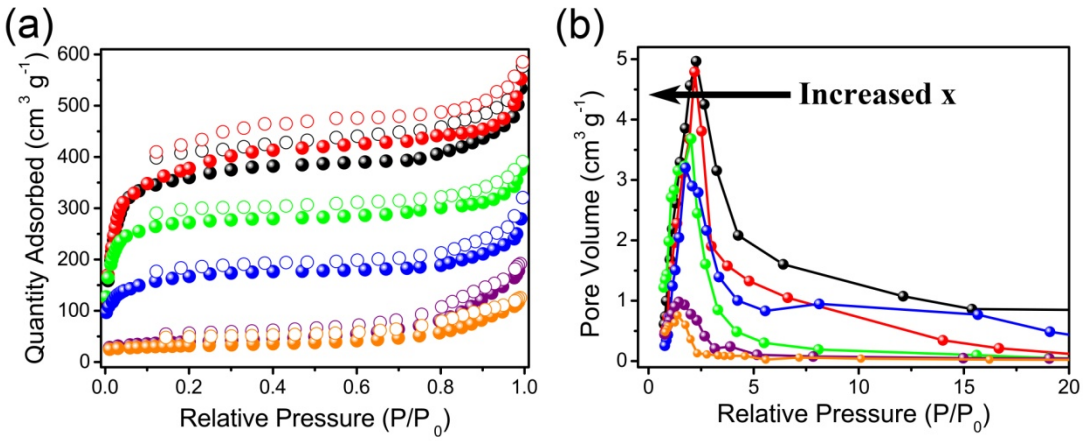

Fig. S4. (a) N_2 adsorption-desorption isotherms and (b) corresponding pore-size distribution curve of Fe-COF (black), B-COF (red), L-His_{25}@Fe-COF (green), L-His_{50}@Fe-COF (blue), L-His_{75}@Fe-COF (purple) and L-His_{100}@Fe-COF (orange).

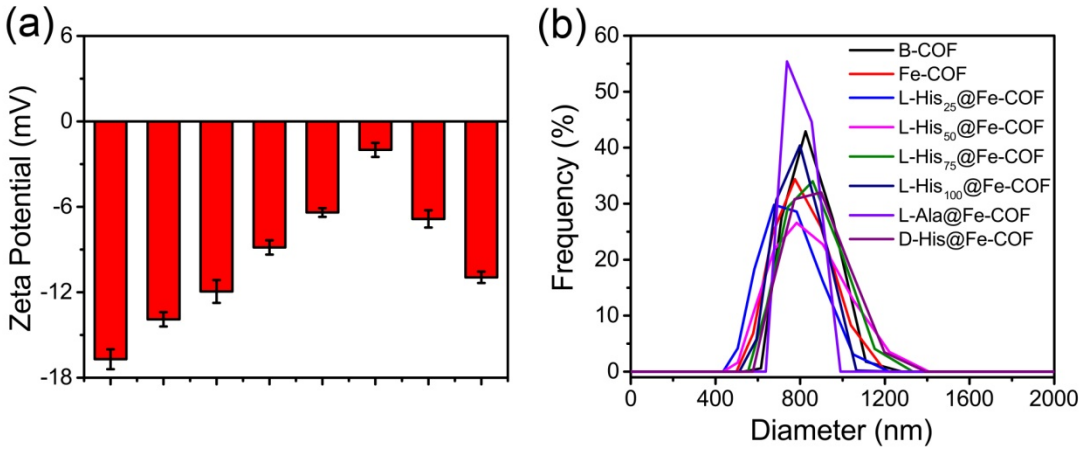

Fig. S5. (a) The results of Zeta potential measurements. Columns from left to right refer to B-COF, Fe-COF, L-His_{25}@Fe-COF, L-His_{50}@Fe-COF, L-His_{75}@Fe-COF, L-His_{100}@Fe-COF, D-His@Fe-COF and L-Ala@Fe-COF, respectively. (b) DLS measure of different kinds of COFs.

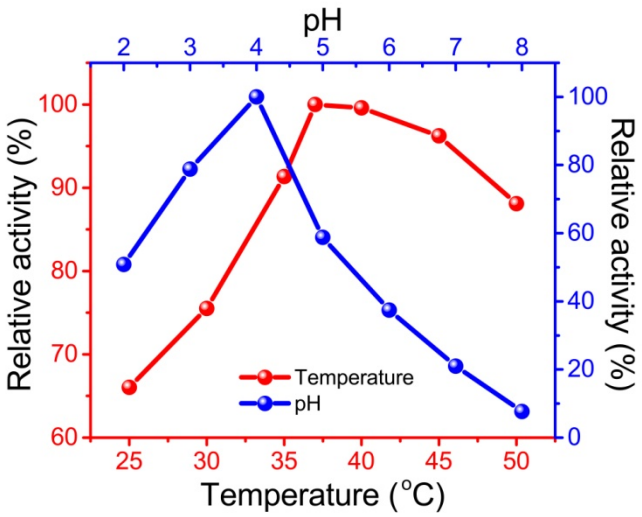

Fig. S6. Peroxidase-like activity of L-His_{50}@Fe-COF is dependent on temperature and pH. Experiments were carried out using 0.9 μg mL^{-1} L-His_{50}@Fe-COF in a reaction volume of 0.5 mL in 25 mM Na_2HPO_4 buffer, 50 mM H_2O_2 and 2.5 mM ABTS at different temperature (pH fixed at 4) or pH (temperature fixed at 37 °C).

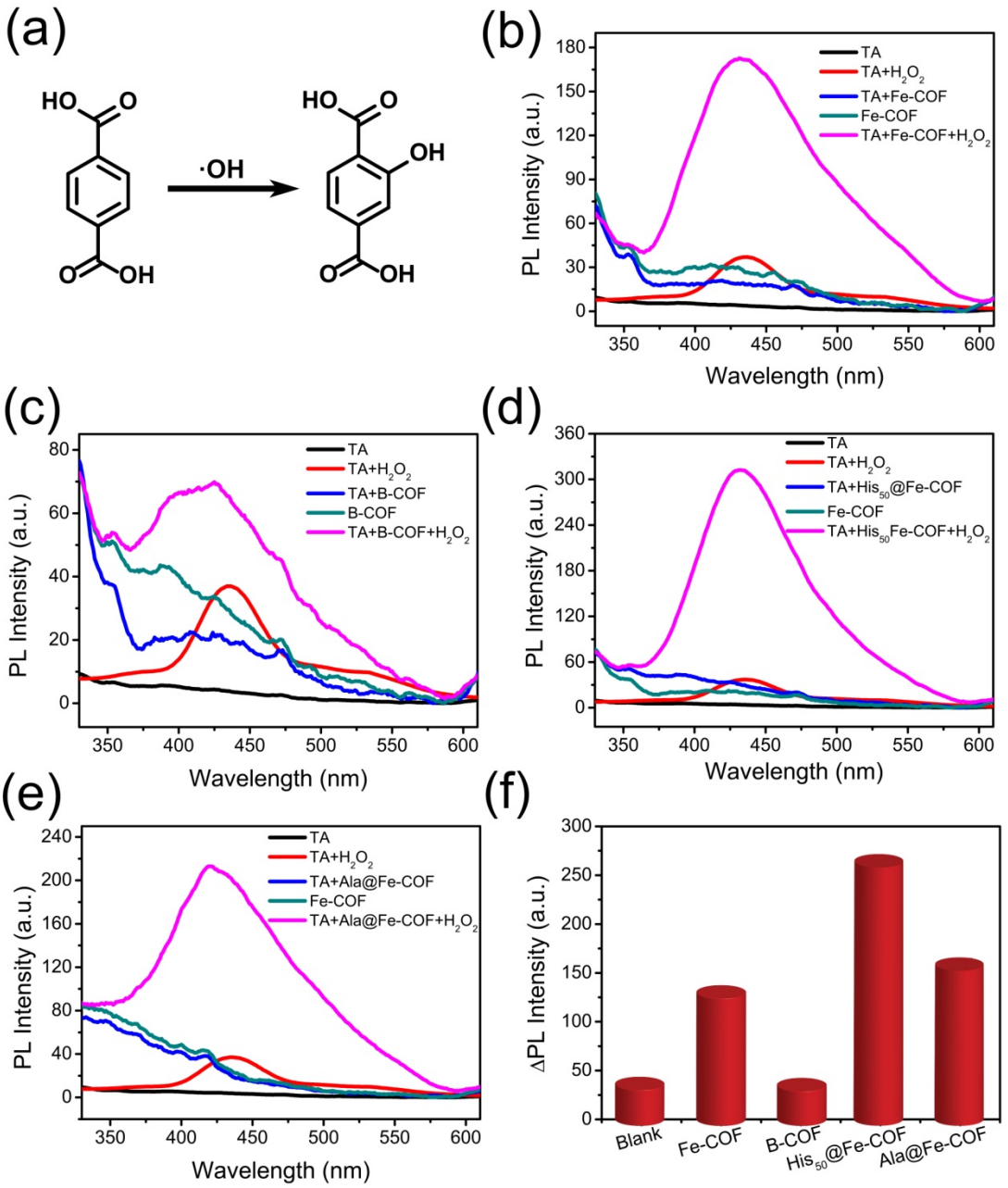

Fig. S7. (a) The reaction between a hydroxyl radical and terephthalic acid (TA). (b-e) Fluorescence spectra of weakly acidic PBS solutions (pH 6.0, 25 mM) containing only TA, TA and H_2O_2, only COFs, TA and COFs, or TA and COFs and H_2O_2 after a reaction time of 24 h. The TA, H_2O_2, and COFs concentrations were 0.5 mM, 1mM, and 0.9 μg mL^{-1}, respectively. (f) Histograms of the changes in photoluminescence intensity (DPL) show the catalytic effect of the different COFs.

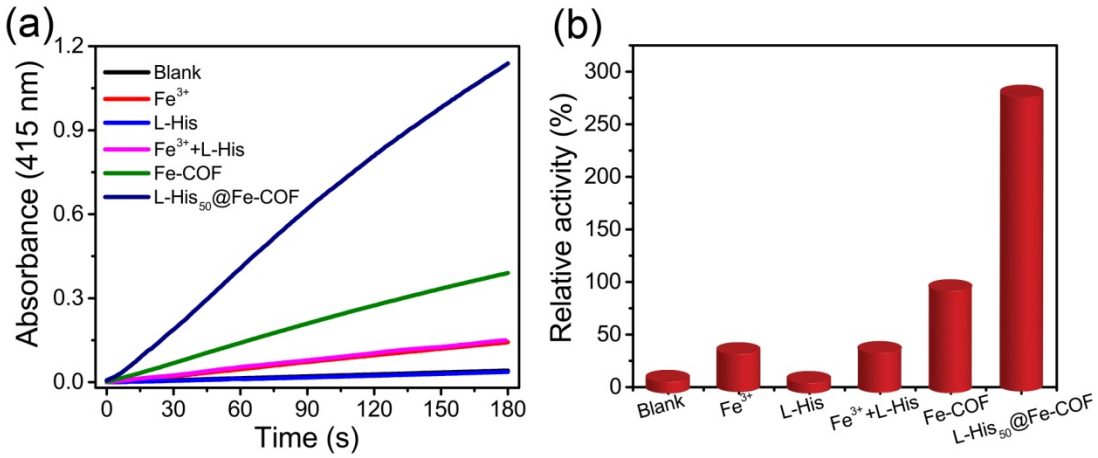

Fig. S8. (a) The time-dependent absorbance changes of ABTS at 415 nm in the presence of different additives. (b) The absorbance at 415 nm after a 3 min enzymatic reaction with different additives. Experiments were carried out in a reaction volume of 0.5 mL in 25 mM Na_2HPO_4 buffer (pH 4.0, 37 °C), with 2.5 mM ABTS and 50 mM H_2O_2. The concentration for COFs, $FeCl_3 \cdot 6H_2O$ and L-His was 0.9 μg mL^{-1}, 4.7 μg mL^{-1} and 2.7 μg mL^{-1}, respectively.

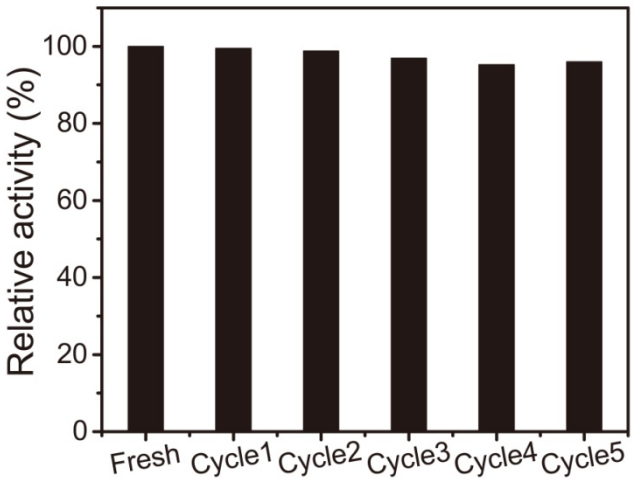

Fig. S9. Recycle test of L-His_{50}@Fe-COF in the oxidation of ABTS.

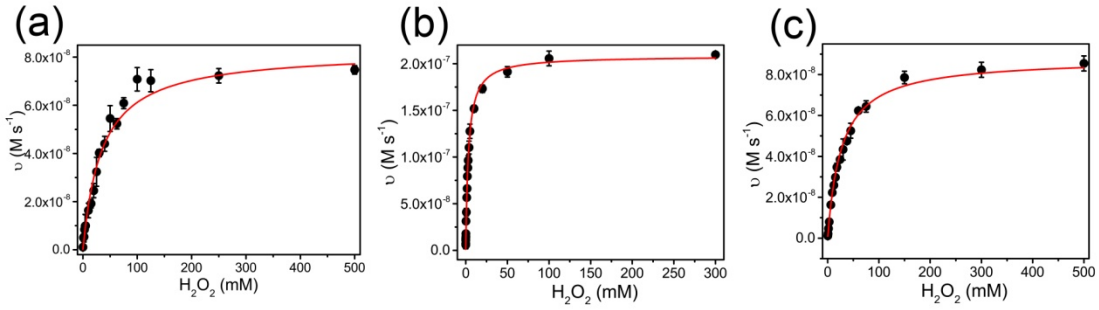

Fig. S10. Saturation curves corresponding to the decomposition of H_2O_2 with the presence of (a) Fe-COF, (b) L-His_{50}@Fe-COF or (c) L-Ala@Fe-COF. Experiments were carried out using 0.9 μg mL^{-1} COFs in a reaction volume of 0.5 mL in 25 mM Na_2HPO_4 buffer (pH 4.0, 37 °C), and 2.5 mM ABTS, with different concentration H_2O_2. Error bars shown represent the standard error derived from three repeated measurements.

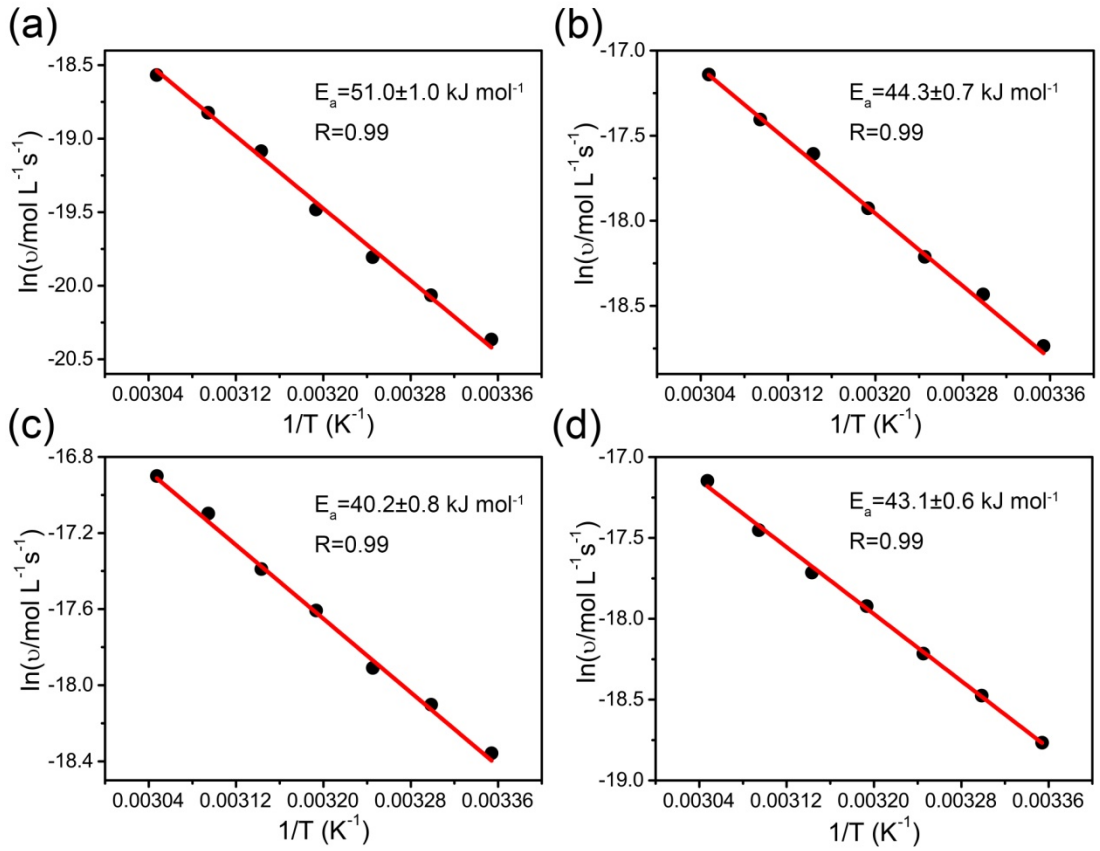

Fig. S11. Logarithmic reaction rate of ABTS oxidation by H_2O_2 with (a) blank, (b) Fe-COF, (c) L-His_{50}@Fe-COF or (d) L-Ala@Fe-COF as a function of reciprocal temperature.

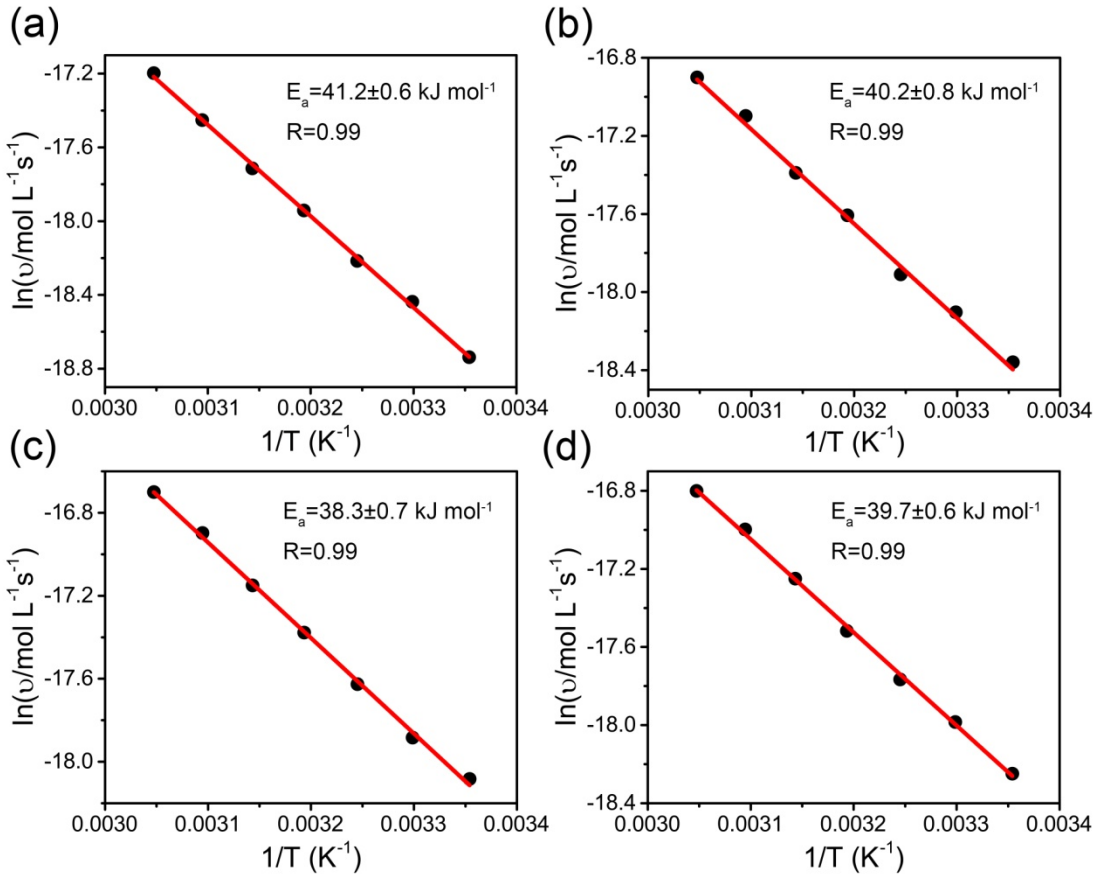

Fig. S12. Logarithmic reaction rate of ABTS oxidation by H_2O_2 with (a) L-His_{25}@Fe-COF, (b) L-His_{50}@Fe-COF, (c) L-His_{75}@Fe-COF or (d) L-His_{100}@Fe-COF as a function of reciprocal temperature.

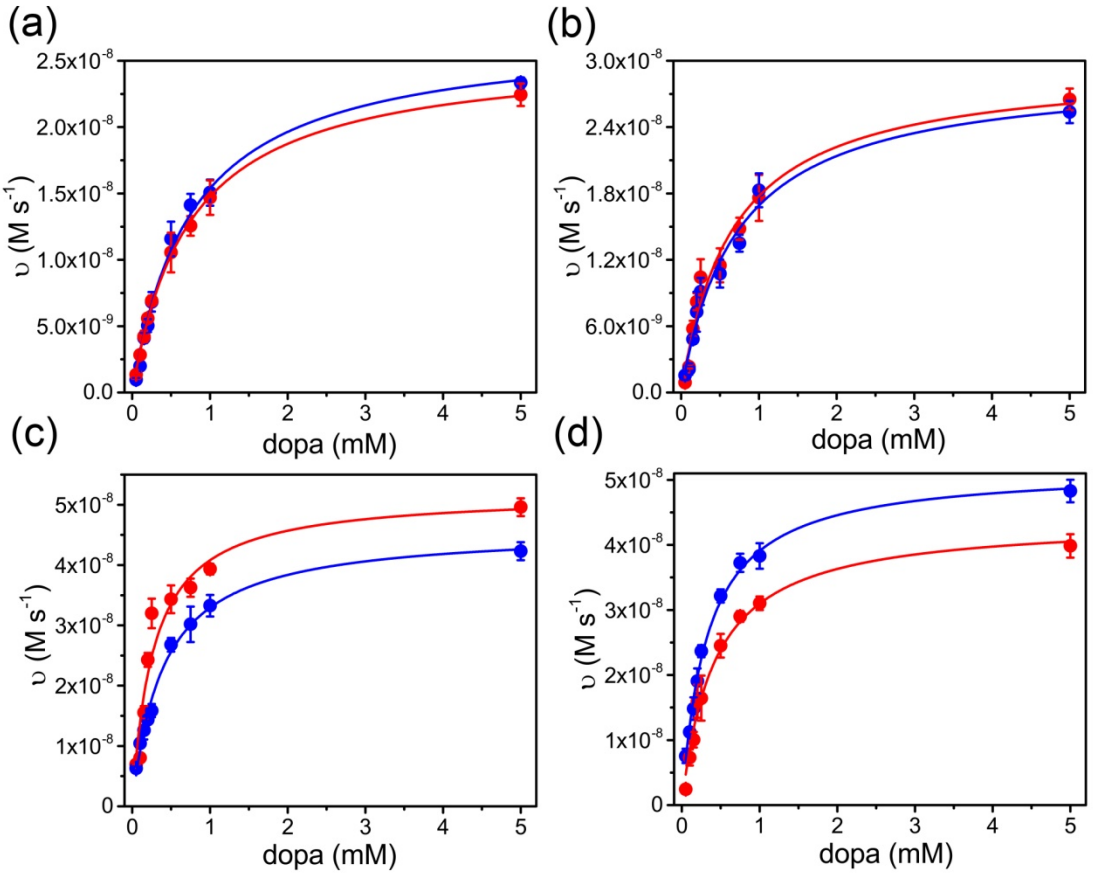

Fig. S13. Saturation curves corresponding to the oxidation of L-dopa (red) and D-dopa (blue) with the presence of (a) Fe-COF, (b) L-Ala@Fe-COF, (c) L-His_{75}@Fe-COF or (d) D-His@Fe-COF. Experiments were carried out using 0.9 μg mL^{-1} COFs in a reaction volume of 0.5 mL in 25 mM Na_2HPO_4 buffer (pH 4.0, 37 °C), and 50 mM H_2O_2, with different concentration dopa. Error bars shown represent the standard error derived from three repeated measurements.

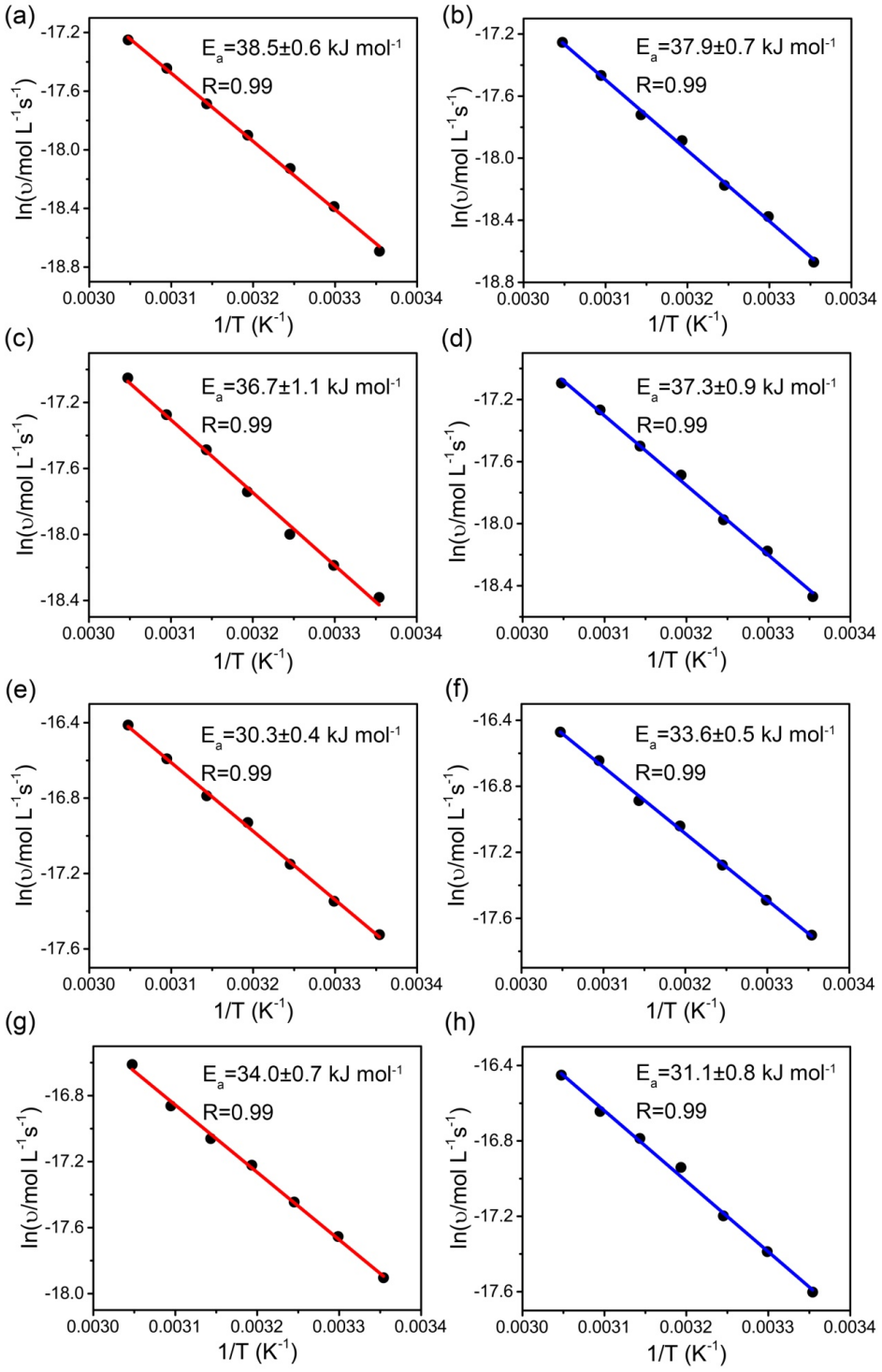

Fig. S14. Logarithmic reaction rate of L-dopa (red) or D-dopa (blue) oxidation by H_2O_2 with Fe-COF (a, b), L-Ala@Fe-COF (c, d), L-His_{75}@Fe-COF (e, f) or D-His@Fe-COF (g, h) as a function of reiprocal temperature.

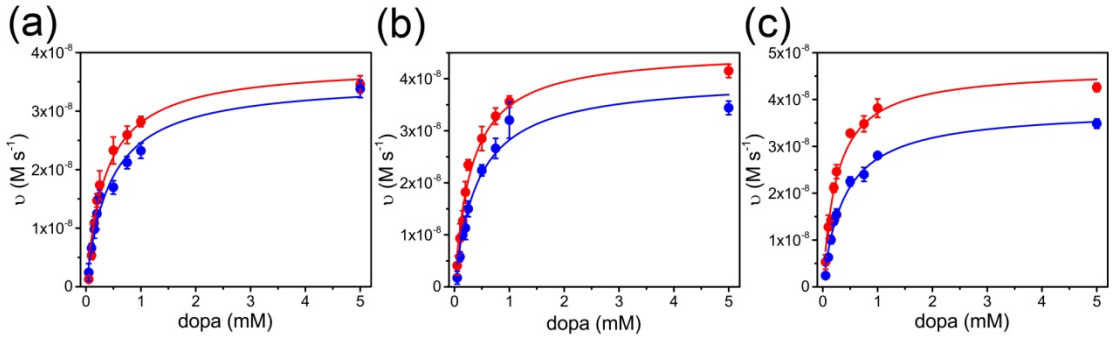

Fig. S15. Saturation curves corresponding to the oxidation of L-dopa (red) and D-dopa (blue) with the presence of (a) L-His_{25}@Fe-COF, (b) L-His_{50}@Fe-COF or (c) L-His_{100}@Fe-COF. Experiments were carried out using 0.9 μg mL^{-1} COFs in a reaction volume of 0.5 mL in 25 mM Na_2HPO_4 buffer (pH 4.0, 37 °C), and 50 mM H_2O_2, with different concentration dopa. Error bars shown represent the standard error derived from three repeated measurements.

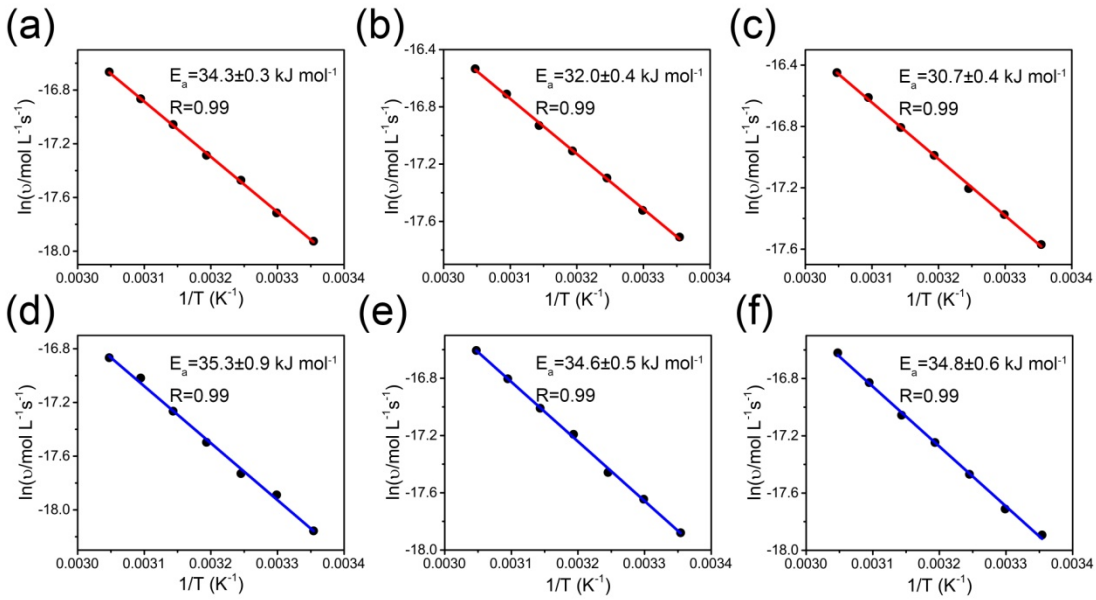

Fig. S16. Logarithmic reaction rate of L-dopa (red) or D-dopa (blue) oxidation by H_2O_2 with L-His_{25}@Fe-COF (a, d), L-His_{50}@Fe-COF (b, e) or L-His_{100}@Fe-COF (c, f) as a function of reiprocal temperature.

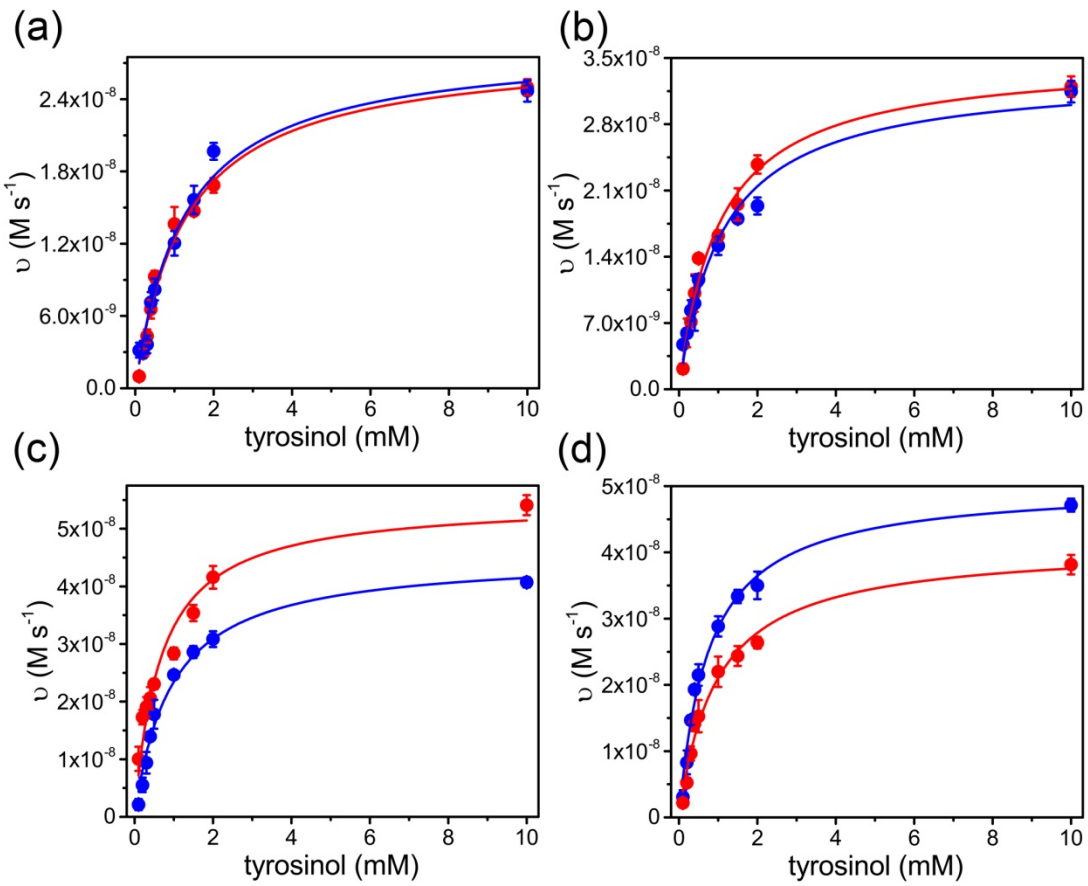

Fig. S17. Saturation curves corresponding to the oxidation of L-tyrosinol (red) and D-tyrosinol (blue) with the presence of (a) Fe-COF, (b) L-Ala@Fe-COF, (c) L-His_{100}@Fe-COF or (d) D-His@Fe-COF. Experiments were carried out using 0.9 μg mL^{-1} COFs in a reaction volume of 0.5 mL in 25 mM Na_2HPO_4 buffer (pH 4.0, 37 °C), and 50 mM H_2O_2, with different concentration tyrosinol. Error bars shown represent the standard error derived from three repeated measurements. The detailed kinetic parameters were shown in Table S5.

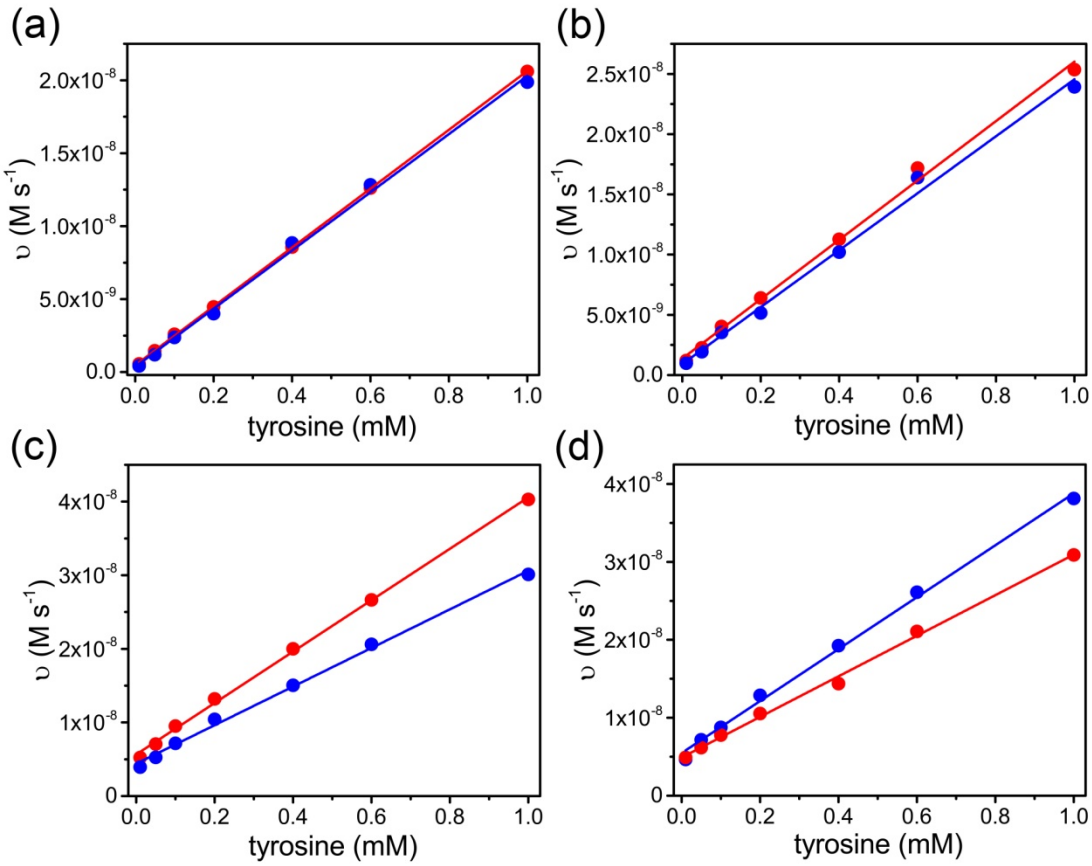

Fig. S18. Steady-state rate (v) vs. the concentration of L-tyrosine (red) and D-tyrosine (blue) with the presence of (a) Fe-COF, (b) L-Ala@Fe-COF, (c) L-His_{100}@Fe-COF or (d) D-His@Fe-COF. Experiments were carried out using 0.9 μg mL^{-1} COFs in a reaction volume of 0.5 mL in 25 mM Na_2HPO_4 buffer (pH 4.0, 37 °C), and 50 mM H_2O_2, with different concentration tyrosine.

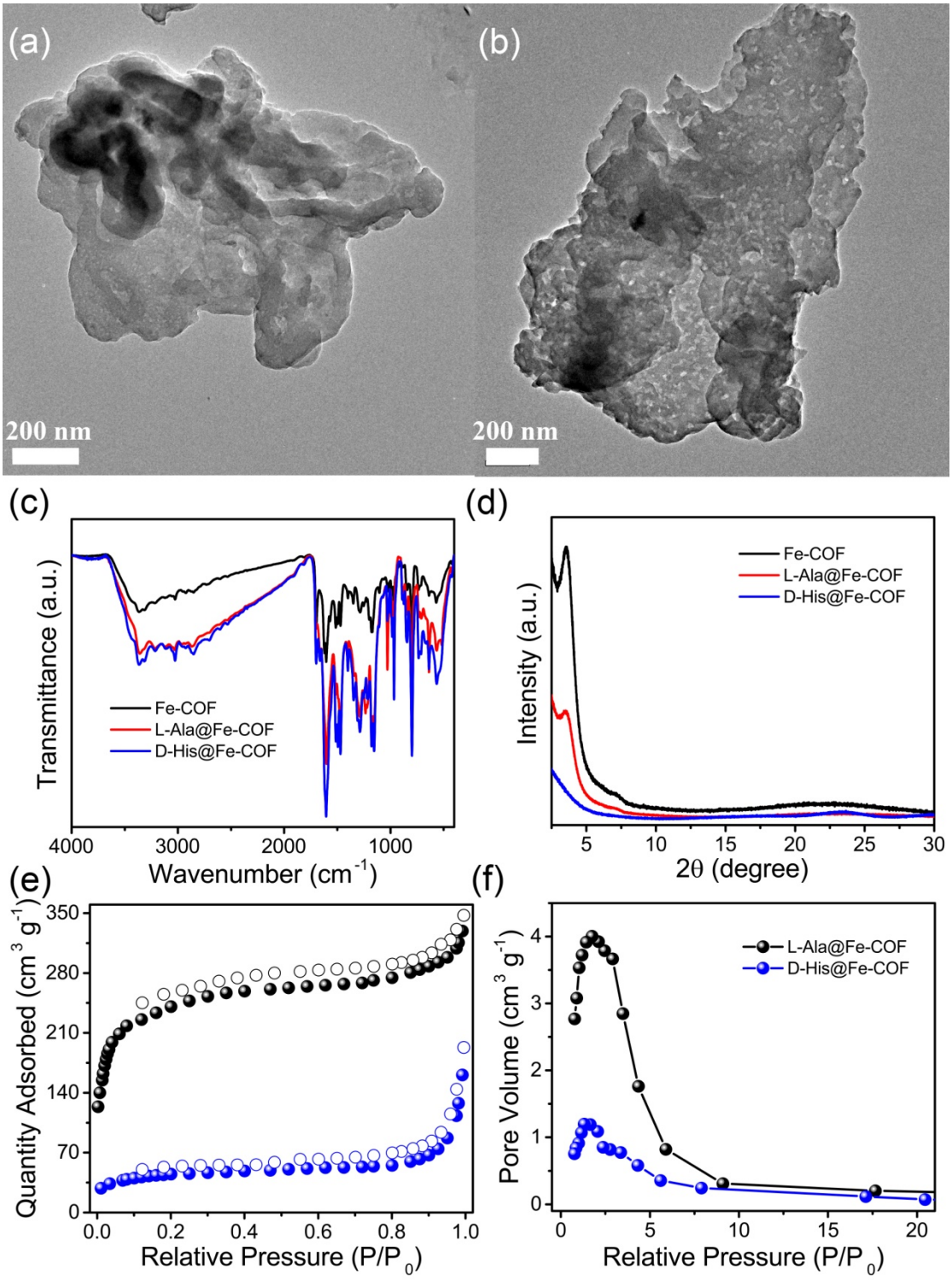

Fig. S19. TEM images for (a) L-Ala@Fe-COF and (b) D-His@Fe-COF. (c) FTIR spectra, (d) XRD pattern, (e) N_2 adsorption-desorption isotherms and (f) corresponding pore-size distribution curve of L-Ala@Fe-COF (black) and D-His@Fe-COF (blue).

The TEM images for L-Ala@Fe-COF and D-His@Fe-COF showed sheet-like morphology, similar to that for Fe-COF and L-His_x@Fe-COF. The FTIR spectra displayed increased vibrations around 3350 cm^{-1} and 3100-3300 cm^{-1}, which could be assigned to the amine groups and the formation of acylamino groups, confirmed the successfully incorporation of the amino acids. The FTIR spectra for D-His@Fe-COF displayed increased peaks at 1700 cm^{-1} due to the imidazole groups in D-His. The XRD pattern of the L-Ala@Fe-COF and D-His@Fe-COF was similar to L-His_{50}@Fe-COF and L-His_{75}@Fe-COF, respectively, confirmed their same crystalline structures as corresponding L-His_x@Fe-COF. The incorporation of L-Ala and D-His resulted in decreased Brunauer-Emmett-Teller (BET) surface area and pore sizes, which was similar to L-His_{50}@Fe-COF and L-His_{75}@Fe-COF, respectively.

Reference:

(1) H. Xu, X. Chen, J. Gao, J. B. Lin, M. Addicoat, S. Irle and D. L. Jiang, *Chem. Commun.*, 2014, **50**, 1292-1294.

(2) S. Mitra, H. S. Sasmal, T. Kundu, S. Kandambeth, K. Math, D. D. Diaz and R. Banerjee, *J. Am. Chem. Soc.*, 2017, **139**, 4513-4520.

(3) M. A. Gilabert, L. G. Fenoll, F. Garcia-Molina, P. A. Garcia-Ruiz, J. Tudela, F. Garcia-Canovas and J. N. Rodriguez-Lopez, *Biol. Chem.*, 2004, **385**, 1177-1184.

(4) H. J. Sun, A. D. Zhao, N. Gao, K. Li, J. S. Ren and X. G. Qu, *Angew. Chem. Int. Ed.* 2015, **54**, 7176-7180.

(5) E. Golub, H. B. Albada, W. C. Liao, Y. Biniuri and I. Willner, *J. Am. Chem. Soc.* 2016, **138**, 164-172.

(6) M. Menzinger and R. Wolfgang, *Angew. Chem. Int. Ed.* 1969, **8**, 438-+.

(7) X. G. Qu, J. O. Trent, I. Fokt, W. Priebe and J. B. Chaires, *Proc. Natl. Acad. Sci. U. S. A.* 2000, **97**, 12032-12037.